Electron-Transfer Dynamics at GaAs Surface Quantum Wells

Sabrina J. Diol

Center for Photoinduced Charge Transfer, University of Rochester, Rochester, New York 14627

E. Poles

Raymond and Beverly Sackler Faculty of Exact Sciences, School of Chemistry, Tel Aviv University, Ramat Aviv 69978, Israel

Y. Rosenwaks

Department of Physical Electronics, Faculty of Engineering, Tel Aviv University, Ramat Aviv 69978, Israel

R. J. Dwayne Miller*

Departments of Chemistry and Physics, 60 St. George St., University of Toronto, Toronto, Ontario, M5S 1A7 Canada

Received: March 2, 1998; In Final Form: June 1, 1998

Interfacial electron-transfer dynamics have been characterized for a heterogeneous semiconductor−liquid junction. Molecular beam epitaxy was used to grow As-capped GaAs (100) surface quantum wells. Removal of the As layer created a pristine, low defect, surface which was studied in situ in direct contact with an outer-sphere, ferrocene, redox couple using time-correlated single photon counting. The surface quantum well structure was used specifically to remove field-dependent transport effects from the photocarrier dynamics. Concentration-dependent decay profiles indicate that a significant fraction of electrons undergo electron transfer. A fit to the data gives an electron-transfer cross section of $(2.4 \pm 0.8) \times 10^{-15}$ cm^2, which corresponds to charge transfer in the adiabatic coupling regime. This work illustrates that the electronic coupling between the solid state and molecular states at the surface can be sufficiently strong to produce adiabatic reaction conditions even for weakly physisorbed outer-sphere acceptors.

I. Introduction

Interfacial charge transfer is a fundamental reaction in surface chemistry. It also forms the core of numerous technologies such as solid-state devices, xerography, photography, and surface-mediated catalysis.[1−5] Over the past several decades, research communities have devoted a great deal of effort toward forming a complete understanding of this basic process.[5] However, advances in this field have been slow due to the inherent difficulties and often fast dynamics associated with surface studies. Consequently, to date, our knowledge of heterogeneous charge transfer significantly lags that of homogeneous electron transfer.

From a fundamental standpoint, the most basic issue with respect to interfacial charge transfer is the degree of wave function overlap between the spatially extended electronic levels of the solid state and the localized, more discrete, electronic states of the molecular acceptors/donors. Within this basis, the degree of overlap determines the strength of the electronic coupling and the crossing probability from the reactant to product surface at the reaction saddle point. For homogeneous (solution) charge-transfer processes, the electronic coupling is invariably in the weak or nonadiabatic coupling regime.[6] The only exceptions are a few photoinduced processes involving charge-transfer bands or intramolecular charge transfer.[7] In contrast at surfaces, there is a dense manifold of electronic levels which can serve as donor/acceptor levels to the reaction coordinate. The high density of occupied electronic states at metal surfaces is expected to enhance the effective electronic coupling.[8,9] This enhanced coupling could lead more generally to adiabatic reaction conditions than that possible for homogeneous electron transfer.[5,9]

Despite the high electronic level density, most theories treat interfacial charge transfer in the weak coupling limit.[10,11] This limit is simpler to treat theoretically, and until recently, there had been no compelling experimental evidence to suggest that strong electronic coupling conditions could occur at surfaces,[12] much less prevail at surfaces. The dearth of experimental evidence for adiabatic coupling conditions could be taken as surprising given that the magnitude of the electronic coupling required for unit transmission probability at the curve crossing region (adiabatic conditions) is relatively modest. The adiabatic limit is defined by the associated nuclear time scale but is typically less than 100 cm^{-1}.[5,13] Based on average electronic coupling parameters found for self-exchange reactions, a straightforward analysis, taking into account the additional electronic levels at a metal surface, suggests that adiabatic electronic coupling should be found as a general feature of surface processes.[9] Experimentally, it is very difficult to probe this issue using conventional electrochemical methods as the observable is usually determined by the rate-determining step in the overall electrochemical cell. It is exceedingly difficult to ensure that the observable is only determined by the interfacial

* To whom correspondence should be sent.

S1089-5647(98)01341-8 CCC: $15.00
Published on Web 07/18/1998

charge-transfer process.[14] However, this issue can be directly probed using time domain spectroscopies.[12] The onset of adiabatic coupling is manifest by electron-transfer dynamics that occur on time scales equivalent to the nuclear relaxation dynamics. For solid−liquid interfaces, the solvent undergoes the greatest repolarization such that the dynamics are largely determined by the solvent coordinate.[5] A correspondence between the electron-transfer dynamics and the solvent dynamics can be made to determine qualitatively if the reaction process involves the strong electronic coupling limit. Alternatively, the relative degree of electronic coupling can be determined from electron-transfer cross sections (vide infra).

The semiconductor−liquid interface offers an ideal system for probing the interfacial charge-transfer dynamics in situ with time-resolved optical experiments. With the appropriate choice of semiconductor interface, the use of short optical pulses enables the creation of a nonequilibrium condition in which excess electrons are prepared spatially within wave function overlap of the molecular acceptors and energetically near the adiabatic crossing point.[12,15] The ensuing dynamics of the photogenerated carrier population gives a direct measurement of the operating time scales involved in interfacial charge transfer. Previously, we have shown that electron transfer to strongly adsorbed inner-sphere acceptors can occur near the adiabatic limit. Specifically, interfacial hole transfer at GaAs-(100)/$Se^{2-/1-}$ aqueous contacts was found to occur within 1−2 ps.[16] This time scale is faster than the diffusive relaxation time of water under the high ionic concentration conditions present at the interface and is uncorrected for carrier scattering to unreactive phase (*k* and *r*) space. To determine whether this observation is a general phenomenon, electron-transfer dynamics involving weakly physisorbed (outer-sphere) acceptors need to be studied. This study is also technologically important as weakly physisorbed outer-sphere acceptors are usually employed for better mass transport and higher currents in photoelectrochemical cells.

It is difficult to rigorously define an outer-sphere donor or acceptor as there is always some inner-sphere reorganization energy associated with a change in charge distribution. The ferrocene (Fc)/ferrocenium (Fc^+) redox couple is considered to be one of the classic examples of an outer-sphere system.[5] Rosenwaks et al. have conducted experiments on p-GaAs/ $Fc^{+/0}$ where the semiconductor was sulfide passivated to reduce recombination through midgap surface states.[17] The Fc^+ acceptor distribution is nearly ideally situated energetically, relative to the conduction band edge for electron transfer. The characteristic electron-transfer time scales were found to be very fast for this surface, with electron-transfer velocities ranging from 10^5 to 10^6 cm/s at 1 mM concentrations. These experiments are complicated by surface field effects on radiative recombination rates and specific surface chemistry that leads to increased surface adsorption of acceptors. It is desirable to avoid surface treatments that might affect the electronic coupling at the interface and to completely eliminate surface field effects on radiative recombination and carrier transport to the surface. To this end, we used molecular beam epitaxy (MBE) to grow a GaAs(100) surface quantum well structure that was capped with As. Removal of the As cap under inert conditions produces a pristine, nearly atomically flat, surface with low surface defects. The quantum confinement, imposed by a barrier layer, eliminates transport normal to the surface and possible transient field gradients from affecting the surface density of photogenerated carriers and radiative recombination. In addition, the radiative emission from the surface quantum well is shifted from the bulk contributions such that the surface carrier population can be selectively studied with high sensitivity using time-correlated single photon counting. Thus, the GaAs(100) surface quantum well/$Fc^{+/0}$ liquid contact represents an ideal system for investigating the fundamental limits to the electronic coupling question.

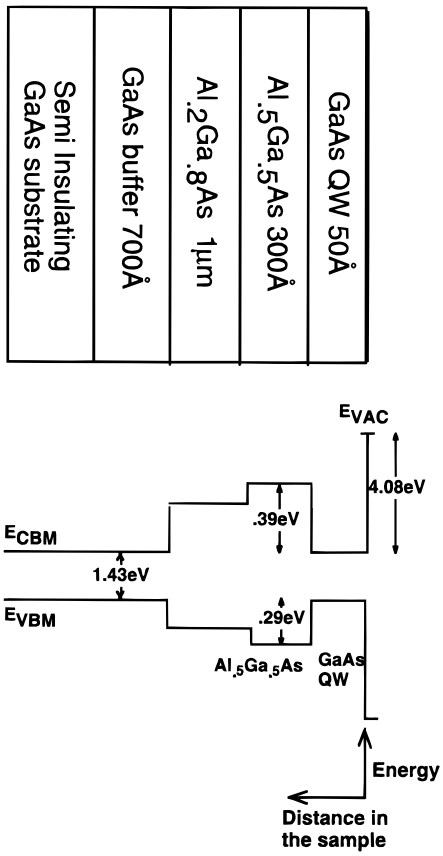

Figure 1. GaAs (100) surface quantum well: sample structure.

II. Experimental Section

The GaAs structure designed for these studies is shown schematically in Figure 1. Semi-insulating GaAs (100) was used as the substrate followed by a 700 Å GaAs layer. A 1 μm $Al_{0.2}Ga_{0.8}As$ buffer layer was specifically incorporated into the design to absorb excitation that would not be quenched by the GaAs surface quantum well, and a 300 Å $Al_{0.5}Ga_{0.5}As$ buffer was chosen to provide maximal energy quantization at the GaAs/ $Al_{0.5}Ga_{0.5}As$ interface. This feature gives the largest barrier to carrier transport in to and out of the surface quantum well region. The GaAs quantum well was protected with an amorphous arsenic cap. Figure 2 shows the steady-state photoluminescence spectrum obtained at room temperature with 524.5 nm excitation using an argon ion laser. The peak centered at 795 nm is from the GaAs surface quantum well, while the peak at 710 nm is from the underlying $Al_{0.2}Ga_{0.8}As$ buffer. There is clearly no signal from the semi-insulating GaAs substrate. Hence, the signal from the surface quantum well is well isolated. To ensure that the sample was properly capped with As prior to the experiment, the sample was placed in an ultrahigh-vacuum chamber to obtain X-ray photoemission spectra, which showed signal from As only (and not Ga). Under ultrahigh-vacuum conditions, the As cap was removed by heating the semiconductor[18] to 450−500 °C, and the surface was checked with photoemission spectroscopy to ensure that the As layer was removed. These surfaces have low surface defect densities[18]

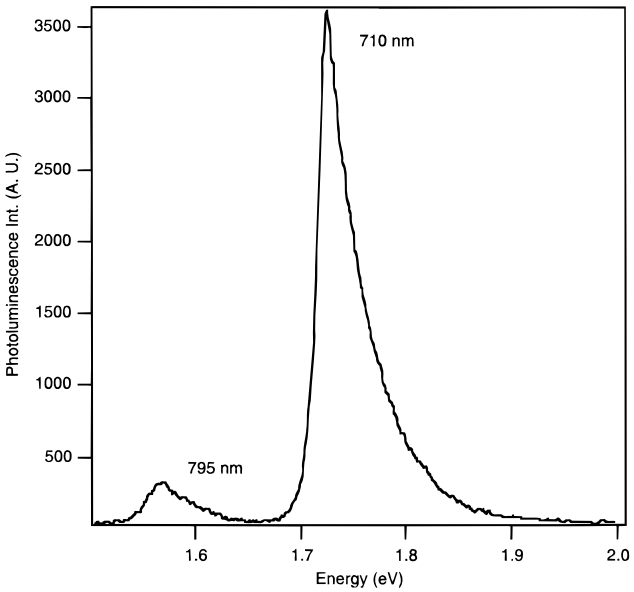

Figure 2. Photoluminescence spectra of 50 Å GaAs quantum well capped with $Al_{0.5}Ga_{0.5}As$.

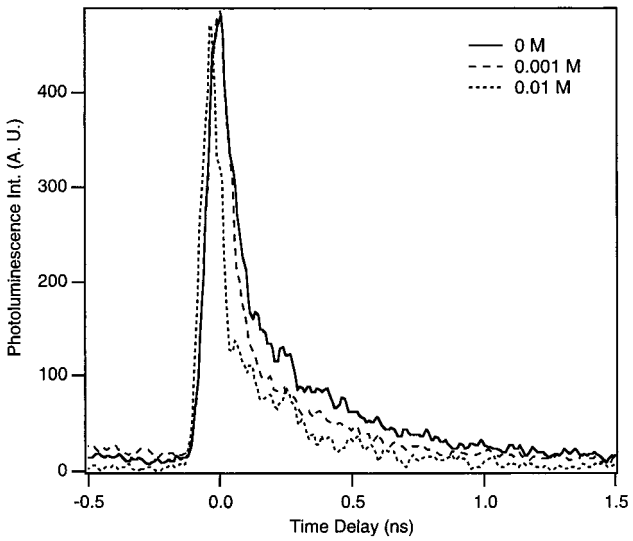

Figure 3. Dependence of the quantum well photoluminescence on the concentration of $Fc^{+/0}$. The dashed line corresponding to 0.01 M $Fc^{+/0}$ has been offset horizontally relative to the other concentrations for clarity.

which was confirmed for the present samples with two-photon photoemission studies and time-resolved carrier recombination. For the photoelectrochemical experiments, the As-capped samples were placed in a high-vacuum cell, which was specially designed to establish a semiconductor/liquid junction. After removing the As capping layer and letting the sample cool under high vacuum, neat anhydrous acetonitrile (CH_3CN) solvent was injected through a fill port. The cell volume was kept as small as possible to minimize the effects of any residual impurities from contaminating the surface. The surface defect density, even in the presence of the liquid, is low enough that interfacial electron transfer becomes the dominant nonradiative channel competing with radiative carrier recombination. In addition, with this procedure, the surface is never exposed to the air to avoid oxide formation which would act as a barrier to the wave function overlap between the molecular acceptors and the surface. The acceptors are able to come into intimate contact with the surface. As a control, the identical GaAs structure was grown except that the final 50 Å GaAs layer was capped with an $Al_{0.5}Ga_{0.5}As$ layer to provide a low defect interface. This latter structure was used to determine the background carrier dynamics in the absence of electron transfer.

The $Fc^{+/0}$ redox couple was constructed using the previous procedure of Rosenwaks et al.[17] Ferrocenium tetrafluoroborate ($Fc^+BF_4^-$) was purchased from the Aldrich Chemical Co. It was purified by recrystallization. Solutions, 0.001 and 0.01 M, were prepared with anhydrous acetonitrile in an oxygen-free nitrogen glovebox. All solution transfers to the photoelectrochemical cell were made in the glovebox. The absorption spectra of the solution was negligible in the region of interest, i.e., around 795 nm where the GaAs surface quantum well emits. Hence, measurement of the GaAs photoluminescence would not be quenched by the electrolytic overlayer. To ensure that the solution would not contribute to the photoluminescence, the steady-state spectra was also measured under the same excitation conditions. Here again, the emission was essentially absent around 795 nm. Hence, any interfering effects from solution emission are also avoided.

Time-correlated single-photon counting was conducted using a standard system with a synchronously pumped and acoustooptically cavity dumped dye laser, as described previously.[15] The time-dependent radiative decay profiles of the GaAs samples were repeated for various concentrations of the outer-sphere acceptor at the semiconductor interface. The sample was excited with 690−700 nm, 20 ps pulses at 1.9 MHz. A 2 mW beam was focused to a 2 mm diameter spot on the sample to photogenerate 5×10^{10} electrons/(cm^2 pulse) in the surface GaAs layer. The quantum well photoluminescence was collected at 795 nm. An interference filter was placed before the monochromator to ensure only detection of photoluminescence from the sample. The photoexcited electron density was maintained below the molecular acceptor density to avoid depletion of the molecular acceptors at the surface and slow molecular diffusion effects on the dynamics. This level of carrier injection is also low enough to avoid significant transient field effects on the dynamics. Assuming all the electrons transfer with no interfacial hole transfer, the maximum transient surface charge would be $5 \times 10^{10}/cm^2$, which corresponds to a maximum change in the surface potential of less than 0.02 eV (less than kT).[19,20] The decay profiles recover completely between laser shots. No long decay components were detected, and the repetition rate was varied by factors of 2−3 to ensure that there was no laser fluence-dependent contributions. Data acquisition times were varied from several hours to less than 3 h for all the different concentrations. Within the signal-to-noise, there were no discernible changes in the measured dynamics over the different time intervals. This study illustrates that the surface is stable against oxidation or other processes for periods of several hours once the surface is in contact with a liquid. Similar stabilization has been observed for GaAs surfaces after photoinduced dissolution of the oxide layer under solution conditions.[21,22] With longer data acquisition times for a single concentration, it was possible to go to lower injection levels. The data were qualitatively the same, and the above injection level was chosen as a compromise in the time required to complete the experiment before problems in surface degradation could arise.

III. Results and Analysis

The concentration dependence of the photoluminescence decay is shown in Figure 3, where the decays have been normalized with respect to intensity. The solid line is for the case of 0 M acceptors, i.e., only solvent. As molecular acceptors

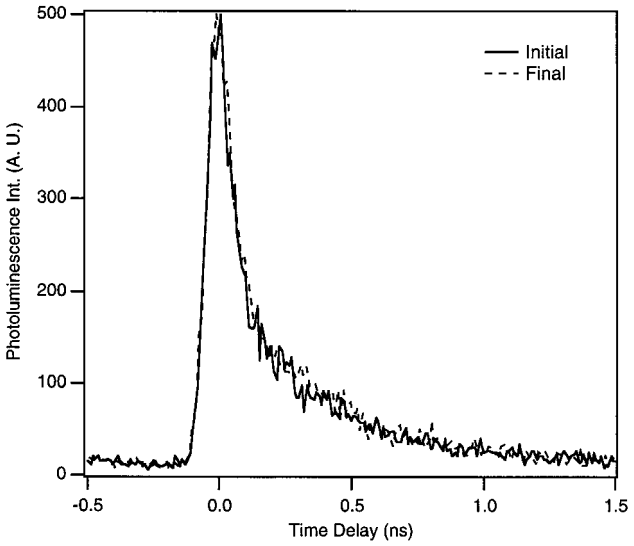

Figure 4. Photoluminescence measurement with only solvent before (solid line, initial) and after (dashed line, final) insertion of molecular acceptor solution.

were added to the solution (0.001 M, dashed line), the photoluminescence became marginally faster. Next this solution was drained out, and 0.01 M $Fc^+BF_4^-$ was inserted. The experimental conditions ensured that the sample surface had the same incident intensity for each measurement. The photoluminescence decay became significantly faster in this case (0.01 M, dotted line) relative to the other concentrations, indicating that the photoexcited electrons in the semiconductor were being depleted quicker. Hence, the more concentrated solution was increasing the branching ratio of the electron-transfer channel to the molecular acceptor relative to the radiative carrier recombination rate. In addition, the correlation of the decay in the carrier population to the ferrocenium concentration demonstrates that this is an electron-transfer process as opposed to hole transfer; i.e., ferrocenium is exclusively an electron acceptor. After the measurement, the 0.01 M solution was drained and the acetonitrile solvent was reinserted. Figure 4 illustrates that the photoluminescence decay was reversible, returning close to the original decay. This indicated that the molecular acceptors were weakly physisorbed on the semiconductor surface, as anticipated for an interface with an outer-sphere acceptor. However, the coupling between the extended band states of the semiconductor and the discrete molecular states is large enough to affect the photoluminescence decay rate.

Under the excitation conditions of the experiment, near flat-band conditions can be assumed. Moreover, even in the case of band bending, field effects would be negligible within the quantum well due to the thin width of the well.[23,24] This greatly facilitates the interpretation of the carrier dynamics in terms of fitting the data to obtain the surface recombination velocity for electron transfer.

To extract quantitative information on the electron-transfer dynamics, the various physical processes affecting the carrier population dynamics need to be included in the analysis. For the case of a single quantum well in contact with an acceptor solution on one side, three main mechanisms that affect the excess carrier density inside the well were considered: (1) electron transfer from the single quantum well to the acceptor in the solution; (2) thermionic emission of electrons from the well to the $Al_{0.5}Ga_{0.5}As$ buffer; (3) recombination processes (radiative and non radiative) inside the well.

The continuity equation for the excess carrier concentration, n, in the well can then be written as[25]

$$\frac{dn}{dt} = -\frac{J_{th}}{ed} - \frac{S_{et} + S}{d}n - R \tag{1}$$

where R is the bulk recombination rate, S_{et} is the electron-transfer velocity to the solution acceptor, S is the surface recombination velocity, e is the electron charge, d is the quantum well width, and J_{th} is the thermionic emission current given by[25]

$$\frac{J_{th}}{ed} = \frac{n}{d}\left[\frac{k_B T}{2\pi m_e^*}\right]^{1/2} \exp(-E_b/k_B T) \tag{2}$$

where E_b is the energy barrier height, m_e^* is the electron effective mass, k_B is the Boltzmann constant, and T is temperature. The bulk recombination rate is given by[26]

$$R = \frac{B\tau n + 1}{\tau}n \tag{3}$$

where B is the radiative rate constant and τ the nonradiative recombination time. These bulk recombination processes were determined by fits to the MBE grown sample with the AlGaAs overlayer. Substituting these expressions in eq 1 gives

$$dn/dt = -jn - Bn^2$$

$$j \equiv \frac{1}{d}\left[\frac{k_B T}{2\pi m_e^*}\right]^{1/2} \exp(-E_b/k_B T) + \frac{S_{et} + S}{d} + \frac{1}{\tau} \tag{4}$$

Equation 4 is a simple form of Bernoulli's equation, whose solution is[27]

$$n(t) = \frac{j \exp(-jt)}{j/n_0 + B(1 - \exp(-jt))} \tag{5}$$

where n_0 is the excess carrier concentration at $t = 0$.

The above equation only considers the electron population dynamics. Since radiative recombination is related to both electron and hole carrier densities, the effect of the holes and the internal electric field generated by changes in the spatial distribution between the electron and hole distributions also needs to be considered. The model needs to include equations for the electrons and the holes and Poisson's equation for the electric field. In addition, a generation function G was introduced to account for electrons and holes injected from the $Al_{0.5}Ga_{0.5}As$ barrier. Thus, the continuity equation for the electrons becomes

$$\frac{dn}{dt} = -\frac{J_{th}}{ed} - \frac{S_{et} + S}{d}n - R + G + \mu_n E n \tag{6}$$

where E is the internal electric field and μ_n the electron mobility. For the holes we obtain

$$\frac{dp}{dt} = -\frac{J_{th}}{ed} - \frac{S}{d}p - R + G - \mu_p E p \tag{7}$$

where p is the excess hole concentration and μ_p the hole mobility; we assume no hole transfer to solution.

The electric field is calculated using the Poisson equation, i.e.,

$$\frac{\partial E}{\partial x} = \frac{q}{\epsilon}(p - n) \tag{8}$$

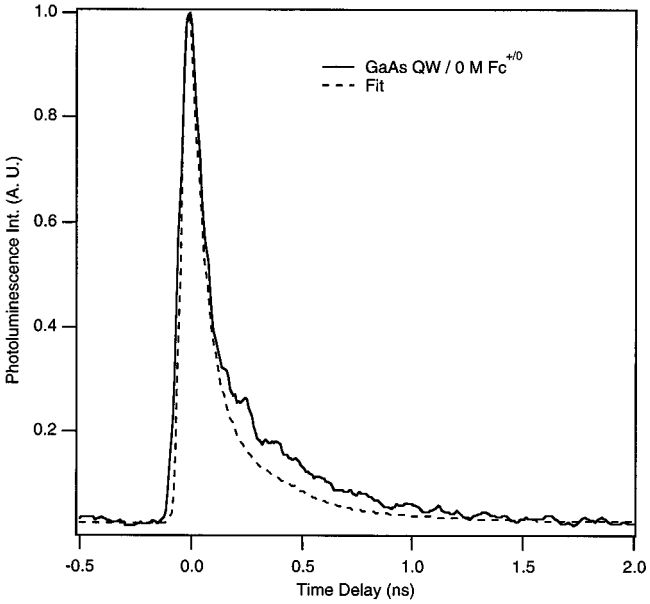

Figure 5. Photoluminescence from GaAs QW/0 M $Fc^{+/0}$ (only acetonitrile solvent) and corresponding fit.

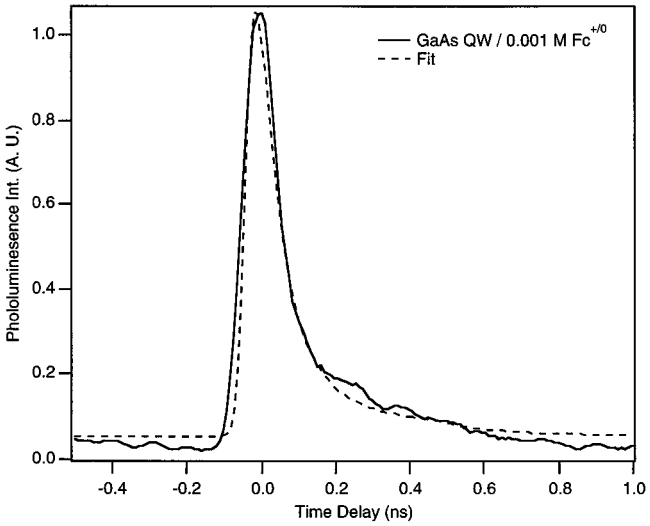

Figure 6. Photoluminescence from GaAs QW/0.001 M $Fc^{+/0}$ and corresponding fit.

where q is the electron charge and ϵ is the dielectric constant of GaAs. In the single quantum well case, one can approximate the electric field derivative and replace it by

$$\frac{\partial E}{\partial x} \approx \frac{E}{d} \tag{9}$$

due to the thickness of the single quantum well region, d.

The set of the three equations (6), (7), and (8) was solved numerically, and the calculated photoluminescence was convoluted with the instrument response function and fitted to the experimental data to yield values for the surface electron-transfer velocity.

Representative fits are graphed in Figures 5−7. For 0 M acceptors (only acetonitrile solvent), the fit depicted in Figure 5 is the control in the absence of electron transfer and corresponds to $S_{et} = 0$ cm/s. Figure 6 illustrates the fitting for a 0.001 M solution where $S_{et} = 1200 \pm 150$ cm/s. For the higher concentration of molecular acceptors (0.01 M), $S_{et} = 7000 \pm 500$ cm/s.

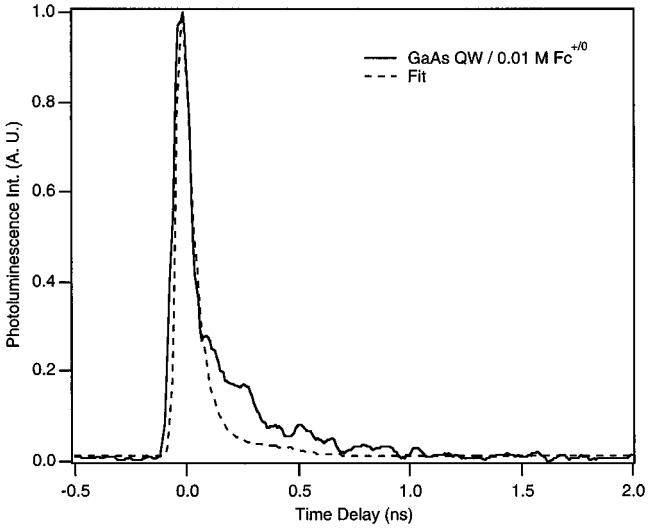

Figure 7. Figure 7. Photoluminescence from GaAs QW/0.01 M $Fc^{+/0}$ and corresponding fit.

The decay in the carrier population due to electron transfer can be related to a two-dimensional cross section that characterizes the electron-transfer process. The relationship is given as

$$S_{et} = \nu_{th}[N_{A^+}]\sigma_{et} \tag{10}$$

where ν_{th} is the electron thermal velocity in the semiconductor half-space, $[N_{A^+}]$ is the concentration of electron acceptors at the interface, and σ_{et} is the electron-transfer cross section. The thermal velocity of the carriers is related to the diffusion constant of the carriers and is well-known for GaAs. Since optical excitation creates both electrons and holes, the diffusion constant of the photocarriers is defined by the ambipolar diffusion constant.[21] The motion of the electron is Coulombically bound to the hole carrier. In this case, the diffusive transport is determined for both carriers by the low mobility hole carrier ($\nu_{th} \sim 1 \times 10^7$ cm/s).[19] The surface concentration of acceptors requires an estimate of the reaction distance. As a starting point, it is reasonable to assume that only those molecules within a diffusion length of the surface, as defined by the photocarrier lifetime, will participate. Only those acceptors that are physically within a few angstroms of the surface will have sufficient wave function overlap to be involved in the electron-transfer process. The photocarrier lifetime ranges between 100 ps and several hundred picoseconds for the different concentrations. Using a diffusion time of 100 ps for a molecule the size of ferrocenium gives a diffusion length of approximately 10 Å[28] and provides an estimate of the reaction distance. Given that the wave function overlap should decay exponentially with a damping constant on the order of 1 $Å^{-1}$, this 10 Å reaction length should be considered an upper limit. The actual number of reactive states will be less than that defined by this volume element. This distance is comparable to the length scale of the Helmholtz double layer at electrodes, such that the cross sections estimated using this reaction length are relevant to the degree of coupling extended to the outer Helmholtz layer. For the 0.001 M solution, this reaction distance gives $[N_{A^+}] = 6 \times 10^{10}$ molecules/cm^2 and for the 0.01 M solution $[N_{A^+}] = 6 \times 10^{11}$ molecules/cm^2. Substituting these values in eq 10 and using the measured electron-transfer velocities gives an average electron-transfer cross section of $(1.6 \pm 0.4) \times 10^{-15}$ cm^2/molecule.

The error bar in this measurement is mainly determined by the assumed reaction distance. The lower limit for the reaction

distance is defined by the molecular diameter. With this reaction distance, only those molecules in contact with the surface are assumed to undergo electron transfer. Assuming weak physisorption and/or a solvation sphere, this latter distance is approximately 5 Å for ferrocenium. With this lower limit, the number of assumed reactive states is a factor of 2 less, and the cross section would need to be correspondingly larger to explain the observed carrier decays. The measured cross sections are considered to be accurate within a factor of 2, as defined by the range of acceptable reaction distances, i.e., $1.6 \times 10^{-15} \leq \sigma_{et} \leq 3.2 \times 10^{-15}$ cm^2/molecule.

This analysis explicitly assumes that there is no significant surface adsorption and that the surface concentration of available acceptors can be estimated from the bulk concentration; i.e., ferrocene is assumed to be weakly physisorbed, and there is no preferential surface adsorption over that of the bulk solvent interaction. It would be desirable to measure the surface concentration independently; however, the degree of sensitivity required for such a measurement is difficult to achieve. With this limitation, the justification for this assumption is based on the following: (1) The surface was prepared under well-controlled conditions to provide a nearly ideal surface with a minimum number of surface states and defects that act as adsorption sites. The defect density for this surface preparation is less than 10^{10}/cm^2 to 10^{11}/cm^2 (less than our detection capabilities with photoemission approaches). The surface state density is at least 2 orders of magnitude smaller than device grade GaAs surfaces[18] and is less than the number density of electron acceptors derived from the bulk solution. (2) The reaction cross section was found to be consistent over an order of magnitude change in concentration, and the magnitude is physically reasonable. The concentration dependence and reversible surface conditions with respect to the carrier dynamics over several hours of repeated investigation indicates that there is no significant adsorption of ferrocenium, beyond weak physisorption.

IV. Discussion

1. Estimates of the Electronic Coupling. The most important parameter extracted from the above analysis is the electron-transfer cross section. This parameter is related to the degree of electronic coupling present at the surface between the extended conduction band electron states and the molecular acceptors. The estimate of the ferrocenium cross section for electron transfer corresponds to a circular surface area of approximately 2−3 Å radius, which is close to the 2 Å axial ring to ring radius of ferrocenium, as defined by the van der Waals surface.[29] In other words, the electron-transfer cross section is in the range of the physical dimensions of the molecular cross section. This finding is significant. It indicates that the electronic coupling at the surface is in the adiabatic, or strong, coupling limit rather than the normally assumed conditions of weak coupling. The degree of adiabaticity defines the probability for electron transfer at the reaction saddle point.[5,6] In the strong coupling limit, there is unit probability for electron transfer at the curve crossing region, whereas in the nonadiabatic, weak, coupling limit the transition probability is much less than unity. The ratio of the reaction cross section to the molecular cross section gives a measure of transition probability and hence the degree of adiabaticity. The above analysis assumes a semiclassical description of the electrons' diffusive motion to the surface reaction plane. This localized basis for the electron wave function can be constructed as a superposition of the eigenstates of the isolated surface quantum well. The cross section is determined using this basis set to describe the degree of mixing of the molecular and solid-state electronic levels. The measured cross section illustrates that once the electron spatially samples the area under the molecule, there is unit probability of electron transfer; i.e., the reaction is adiabatic.

The above range of cross sections corresponds to an area 1.3−2.5 times the molecular diameter and further indicates that the degree of coupling is larger than the minimum required for the adiabatic condition. A larger reaction cross section than the molecular diameter reflects that there are additional surface atoms outside the region in direct contact with ferrocenium that experience sufficient electronic mixing to contribute to an adiabatic passage through the saddle point. Taking the minimum electronic coupling for adiabatic behavior to be 100 cm^{-1} for an acetonitrile liquid interface, the lower estimate for the cross section indicates that the electronic coupling between the ferrocenium and the immediately adjacent surface atoms is at least 100 cm^{-1}. The upper estimate for the electron-transfer cross section corresponds to an area significantly larger than the molecular dimensions and would correspond to a larger electronic coupling with the nearest-neighbor surface atoms than the above minimum electronic mixing of states.

The electronic coupling is related to the wave function overlap between the acceptor and the surface. This overlap decays exponentially from the area defined by the physical dimensions of the molecule. The electron-transfer rate and electron transmission probability depend on the modulus squared of this exponentially decaying overlap integral. With the basis set used in the model to extract the electron-transfer cross section, the electronic coupling (V) distance dependence in the surface plane can be expressed as

$$|V(r)|^2 = |V(r_0)|^2 e^{-\beta(r-r_0)}; \quad r \geq r_0 \tag{11}$$

where the separation between the surface and the acceptor molecule is assumed fixed and r is the distance along the surface plane from the center of the acceptor. The reference (r_0) is defined to be the distance of maximum electronic coupling (closest approach). The electron distribution on ferrocenium is relatively constant in comparison to the exponential damping of the acceptor wave function at distances lying outside the van der Waals surface of the molecule. On this basis, we take r_0 to be the molecular radius as the reference distance defining the maximum electronic mixing with the surface atoms. The damping constant (β) is not well defined but should be approximately 0.85 Å^{-1}. This particular β has been found for a number of systems involving through space coupling.[30] Since the cross section is in the adiabatic limit, the minimum electronic coupling is 100 cm^{-1}, which defines the outer point in this area or the effective radius (r_{eff}) of the capture cross section. To estimate the maximum electronic mixing with the surface at r_0, we need to assign the molecular radius, the value of which depends on the orientation of ferrocenium relative to the surface. The cyclopentadienyl groups define a radius of 1.2 Å in contact with the surface, whereas a surface orientation with the axial ligands of the iron in contact with the surface define a radius of 2 Å for r_0. Using $V(r_{eff}) = 100$ cm^{-1} and the upper limit to the electron-transfer cross section ($r_{eff} = 3.2$ Å), the electronic mixing at the molecular physisorption site would have to be in a range of 160−230 cm^{-1} for these two possible orientations. There are issues in properly defining which state is involved as the electron acceptor level; for example, an Fe-centered d-orbital versus the ligand positions will change the value for r_0 and the decay of the wave function overlap. However, in the current problem the difference of 1 Å does not change this estimate significantly. The observed electron-transfer velocities are

consistent with electronic coupling parameters between the ferrocenium and the surface in a range of 100−200 cm^{-1}.

This estimate does not take into consideration the energetics of the Fc^+ acceptor distribution relative to the $n = 1$ level of the surface quantum well. In principle, the surface concentration of acceptors should be corrected to reflect this distribution. The relative position of the Fc^+ electron acceptors depends on the reorganization energy. Using the experimentally determined value of 0.85 eV for the reorganization energy,[31] the maximum in the distribution lies within 0.03−0.06 eV above the solid-state donor level. These energetics are nearly ideal for this system such that the correction is minor relative to other uncertainties in the estimate. However, this consideration does point out that this estimate is a lower bound, and if there is a nuclear activation barrier, the electronic coupling could be larger.

Future studies using different quantum well thickness to vary the relative position of the $n = 1$ level should prove to be a unique probe of the acceptor distribution. It would also be useful to include explicitly the acceptor spatial distribution and Coulombic effects to better refine the estimates of the electronic coupling. For the present purposes, the above estimate of 100−200 cm^{-1} for the electronic coupling is sufficient within the experimental signal-to-noise and dynamic range.

2. Comparison to Other Estimates of Adiabaticity. The above estimate for the electronic coupling should be compared to other measurements. Electrochemical studies have used self-assembled monolayers (SAM) to form a blocking layer to decrease the electronic coupling with the surface.[31−33] With the increased barrier width, the electron-transfer rate becomes slow enough to become the rate-determining step, and reasonably accurate measurements of the electronic coupling have been made.[33] Collectively, this work has shown that the electron-transfer rate decays exponentially with distance from the surface over several orders of magnitude change in rate constants. The distance is determined by the thickness of the SAM layer and is large enough to ensure that the electronic coupling is in the weak coupling limit. This condition is necessary both to make the experiments tractable and to aid in comparison to theory which is predominantly confined to the assumption of nonadiabatic electron transfer. To correlate the observed heterogeneous rate constants to electronic coupling, one needs the electronic density of states of the electrode surface to properly weight the observed current. The most recent results of Creager et al. have made a reasonably accurate estimate of the relevant electronic density of states by correlating several different, independent, experimental determinations.[33] With this parameter in hand, this work has obtained electronic coupling parameters as large as 6 cm^{-1} for ferrocene-derivatized SAM's on Au(111) separated from the surface by 10 bond lengths.[33] Extrapolating this coupling, using the measured damping constant, to direct contact between ferrocene and the metal surface gives an electronic coupling on the order of 1000 cm^{-1}. There is a problem in making a direct comparison between the present findings and this estimate. The band structure of GaAs is significantly different from Au such that the coupling between Au and ferrocene would not be expected to be the same as that for GaAs. The most important point is that the degree of coupling extrapolated from this work is qualitatively consistent with the above picture; i.e., electron transfer to ferrocene/ferrocenium within the Helmholtz region at an electrode surface occurs within the strong coupling limit. This conclusion is further supported by earlier turbulent flow studies with extremely high flow velocities to avoid mass transport limits on the interfacial current.[14] This study found, for different metals, that the heterogeneous electron-transfer rate constant was independent of the electronic density of states. This finding again indicates at least on a qualitative level that the electronic coupling is adiabatic.

Apart from the fundamental importance of this determination, there are also important practical applications for adiabatic charge-transfer processes. Nozik and co-workers have pointed out previously that if the charge-transfer processes at surfaces could be made to occur faster than photocarrier thermalization, it would be possible to double the theoretical maximum solar energy conversion efficiency to 66% for a single semiconductor liquid junction.[34,35] This hot electron model for surface photochemistry has been the subject of debate.[36] Generally, it has been considered that electron transfer could not occur fast enough to kinetically compete with carrier thermalization. This issue of time scales for interfacial charge transfer reduces to the degree of electronic coupling and the rate of nuclear passage through the curve-crossing region. With proper energetics for the acceptor distribution, photoinduced charge-transfer processes can be optimized to occur under barrierless (nuclear) conditions; i.e., the photon energy supplies the activation energy rather than thermal fluctuations. The nuclear relaxation along the reaction coordinate is largely determined by the solvent coordinate for an outer-sphere acceptor.[5] In the past few years, it has been shown in a wide variety of systems that over half the reorganization energy is determined by the nondiffusive inertial modes of the liquid.[37] For acetonitrile, this solvent component has an effective relaxation time on the order of 100 fs. It is this motion which determines the lower limit to the electron-transfer time for adiabatic coupling (barrierless) conditions. Weaker coupling reduces the transition probability and increases the effective electron-transfer time from this lower limit.

The above work illustrates that the electronic coupling can approach the adiabatic limit; however, the electron-transfer dynamics shown in Figures 3−7 do not exhibit the aforementioned solvent-controlled time scales. Under the low surface concentration conditions of these experiments, the dynamics are determined by electron transport to the reactive sites at the surface. We are currently limited in the surface density of acceptors by the low solubility of ferrocenium tetrafluoroborate in acetonitrile. In principle, the surface concentration can approach monolayer coverage. Rather than repeat the more detailed analysis given above for higher acceptor concentrations, the electron-transfer time from the surface region can be approximated to first order by a one-dimensional diffusion problem with a reactive surface boundary condition. For the structure shown in Figure 1, the 1/e decay time in the electron population due to electron transfer, within this simple approximation, is given by[5]

$$\tau_{et} = d/S_{et} \tag{12}$$

where d is the width of the quantum well. Using the measured surface electron-transfer velocity for the 0.01 M concentration and $d = 50$ Å, the calculated τ_{et} is 70 ps. This calculated decay time is close to the experimental results (1/e decay time of 100 ps), which illustrates that the largest effect on the photoluminescence decay is electron transfer to the solution acceptors. It is also interesting to consider the case of a monolayer coverage of molecular acceptors at the interface, as this represents the lower limit to electron-transfer time scales. This situation corresponds to a two-dimensional concentration of 3.5×10^{14} molecules/cm^2. Substituting this value for the surface density and the median value of $\sigma_{et} = 2 \times 10^{-15}$ cm^2/molecule from the experimental results yields $S_{et} \approx 10^7$cm/s (eq 10). This

electron-transfer velocity is the same as the thermal velocity, which means that as soon as the electron samples the surface region it transfers across the interface. At such a high velocity and high concentration, for $d = 50$ Å, τ_{et} would reduce to around 50 fs. This time scale would correspond to the solvent-controlled dynamics of an adiabatic process. The estimate is highly simplified but does illustrate that the measured cross sections and kinetics are compatible with time scales associated with adiabatic electron-transfer processes.

This work and previous studies of strongly adsorbed acceptors[5,12,16] and weakly physisorbed dyes for semiconductor sensitization[5,12,15] have shown that fundamentally the electronic coupling between discrete molecular states and the extended electronic states of a conducting surface can occur in the strong coupling limit. This information along with a recent, complete, characterization of the electron thermalization dynamics at GaAs(100) surfaces[38] and at the above GaAs structure[39] (in the energy range relevant to surface photochemistry) has shown that the photoinduced electron-transfer dynamics can be competitive with electron thermalization. Thus, the basic tenets of the hot electron model for surface photochemistry are correct. Hot-electron-transfer channels can be a significant surface reaction channel. The manifestation of hot electron chemistry has even been found at metal surfaces for strongly adsorbed states under UHV conditions.[5,40] This finding could be taken as surprising given the extremely fast electron−electron scattering and thermalization that occurs in metals.[41] However, the observation of photoinduced charge transfer at metals further illustrates that the nuclear relaxation dynamics along a reaction channel is reaction specific and can be competitive with solid-state relaxation processes in certain cases.[5] Under UHV conditions, the surface/molecule interaction for a metal is appreciable, and the electronic coupling approaches the adbond energy. For a liquid interface, the interaction of the molecule is not confined to the surface, and the solvation forces should lead to minimum free energy conditions in which the coupling to the surface is reduced. In this context, the distinguishing feature of the present work is that the electronic coupling at a solid/liquid interface can also approach the strong coupling limit with respect to interfacial charge transfer. The fact that this conclusion has been extended to include weakly physisorbed outer-sphere acceptors indicates that heterogeneous electron transfer is more generally in the adiabatic limit, in contrast to homogeneous electron-transfer processes which are found to occur almost exclusively in the nonadiabatic limit.

3. Implications for Electrochemical Processes. This observation has potentially important consequences to understanding electron-transfer processes at electrode surfaces in general. The majority of the work on heterogeneous electron transfer has assumed nonadiabatic processes. This first-order treatment has been very successful in explaining a wide range of electrochemical phenomena extending over several decades in dynamic range.[2−6,8,16] One has to question how a nonadiabatic treatment could properly predict trends if the electronic coupling out to the outer Helmholtz layer is sufficient to produce adiabatic conditions. There are two points to consider. First, we need to consider the effect of the nuclear activation barrier. The electronic coupling is appreciable; however, the above determinations correspond to a reduction in the nuclear activation barrier in the range 0.01−0.1 eV. The heterogeneous electron-transfer rate would still be largely determined by the nuclear activation barrier; i.e., the degree of electronic coupling is in the so-called weakly adiabatic to intermediate adiabatic coupling regime.[5] Furthermore, the reorganization energy (≈1 eV) is not known with sufficient accuracy to draw attention to reductions in the nuclear activation barrier of this magnitude. The reorganization energy is generally calculated or used as a fitting parameter.[5−11,30−33] Thus, the effect of the degree of electronic coupling on the activation barrier, of this magnitude, would not be discernible. Second, the effective reaction distance may be farther removed from the surface than the Helmholtz double layer. One might expect that for activationless conditions (large overpotentials for metal electrodes or proper choice of acceptors for semiconductors) that the adiabatic condition would become apparent in the measured rate constants. However, the translational diffusion of acceptors to the surface reaction plane is relatively slow. If the electron-transfer step at distances farther than 1 nm from the surface is faster than the diffusion time into the adiabatic coupling zone (distances less than 1 nm from the surface), the majority of the electron-transfer processes could occur under nonadiabatic conditions or weakly adiabatic conditions. This is certainly the case. The translational diffusion time for net rms motions of 1 Å for typical solvated acceptors is on the order of 1 ps or slower. Under barrierless conditions, the electron-transfer times for marginally adiabatic conditions are on the picosecond to subpicosecond time scale such that electron transfer would occur before significant penetration into the adiabatic zone. The electron-transfer step to suitable acceptors would occur essentially at the edge of the adiabatic coupling distance, and the concentration gradient in the acceptor distribution would be displaced from the surface to an effective reaction distance that would be consistent with a weak coupling approximation. Basically, the electron-transfer process would occur at distances at which the electronic coupling is relatively weak before the molecule has a chance to diffuse to distances from the surface that would correspond to stronger mixing of electronic states. This microscopic transport effect would be independent of any external perturbation used to remove macroscopic diffusion from limiting the current (rotating disk or turbulent flow). In this manner, the degree of electronic coupling for distances between the surface and acceptors within the Helmholtz layer would not contribute to the transfer rate and would not be probed in conventional electrochemical measurements.

Both the sensitivity of the reaction rate to the nuclear activation barrier and the relative time scale for molecular translational motion versus the distant-dependent electron-transfer rate can account for the general success of nonadiabatic electron-transfer theories. These same phenomena are largely responsible for the observation of nonadiabatic coupling in solution. It is not an issue whether donor/acceptor pairs in solution can exhibit strong enough electronic mixing to correspond to strong coupling conditions for electron transfer. If molecules in solution come into direct contact, the electronic mixing is sufficient to form charge-transfer bands, as exemplified by van der Waals contact pairs.[16,42] In fact, the electronic mixing between electronic manifolds can be significantly larger than the above results for the surface interaction. However, the magnitude of this coupling is still not sufficient to completely eliminate typical nuclear activation barriers. Under these conditions, the nuclear activation barrier still dominates the process. Again, even for systems without an appreciable barrier, the process of translational diffusion into the strong coupling zone would be much slower than the time scale of the nonadiabatic electronic transition. The relative residence time within the adiabatic reaction zone is too short to affect the kinetics. Thus, the overwhelming majority of electron-transfer events in solution occur between solvent-separated molecules at distances well into the weak coupling limit.

4. Distinctions of Photoactivated Electron Transfer. The above discussion serves to rationalize the current observations with those from conventional electrochemical measurements. However, the new insights concerning the degree of electronic interaction between molecules and electrode surfaces also provide a clear distinction between thermal and photoinduced electron-transfer processes at surfaces. In the former case, the reaction rate is determined by nuclear activation barriers and translational molecular diffusion toward the surface that affects the effective reaction distance. In the case of photoinduced processes, the photon energy supplies the activation energy (or a significant fraction thereof), and the transport is now determined by the highly mobile free electron and hole carriers of the solid state. As opposed to molecular diffusion which requires nuclear motion, the spatial mobility of the reactive charge carrier is essentially an electronic process and is orders of magnitude faster than molecular diffusion. The spatial transport and sampling of reactive surface sites by the carriers are now significantly faster than nonadiabatic electronic transitions, and the reaction can proceed under adiabatic conditions. As long as the optical intensities are kept low enough to avoid saturating the available acceptors in direct contact with the surface (within the adiabatic zone), the electron and hole transfer dynamics can occur within the strong coupling limit.

This distinction is important as it changes the relevant time scales assumed to be operating at these interfaces. Traditional views of slow electron-transfer processes within a weak coupling framework are no longer strictly valid. Electron and hole transfer from the band edges, as opposed to surface state mediated, and even hot electron channels become viable reaction pathways. Most notably, the concept of hot electron transfer would be completely inconsistent with a weak coupling treatment adapted from electrochemical studies of electron transfer. The recent observations of femtosecond electron-transfer dynamics at semiconductor[5,12,43−45] and metal surfaces,[40] in relation to electron thermalization,[41] illustrate the inadequacies of the weak coupling approximation. The current findings indicate that significant wave function overlap and electronic mixing at surfaces should be extended to include outer-sphere acceptors. This new fundamental insight may ultimately have important practical applications in the fully optimized engineering of interfaces for solar energy conversion; i.e., both thermalized band edge and hot electron channels can be exploited to minimize energy losses.

Equally important, this distinction means that the quantum aspects of electron transfer at surfaces can be explored and subjected to more detailed theoretical analysis.[46−48] This result also means that time domain studies provide a direct connection to the barrier crossing dynamics at interfaces. To date, the nuclear dynamics determining the rate of passage through the reaction saddle point have only been estimated from studies of bulk liquids.[5,12] The electrode double layer represents a very rarefied environment in which direct studies are required to truly understand the effect of the large fields present at the interface on the transition-state processes. This work illustrates that photoinduced charge transfer at surfaces can be used to uniquely probe this aspect of the problem.

Acknowledgment. This work was supported by the United States Department of Energy and the Natural Sciences and Engineering Research Council of Canada (R.J.D.M.). S.J.D. would like to acknowledge the Link Energy Research Foundation Fellowship.

References and Notes

(1) Fraser, D. A. *The Physics of Semiconductor Devices*, 4th ed.; Oxford University Press: New York, 1986.
(2) Williams, M. *The Physics and Technology of Xerographic Processes*; John Wiley and Sons: New York, 1984.
(3) Dessauer, J. H. *Xerography and Related Processes*; Focal Press: New York, 1965.
(4) James, T. H. *The Theory of the Photographic Process*; MacMillian: New York, 1977.
(5) Miller, R. J. D.; McLendon, G.; Nozik, A.; Willig, F.; Schmickler, W. *Surface Electron-Transfer Processes*; VCH: New York, 1995.
(6) Marcus, R. A.; Sutin, N. *Biochim. Biophys. Acta* **1985**, *811*, 265.
(7) Barbara, P. F.; Jarzeba, W. *Adv. Photochem.* **1990**, *15*, 1.
(8) Marcus, R. A. *J. Chem. Phys.* **1965**, *24*, 966; **1965**, *43*, 679.
(9) Schmickler, W. *J. Electroanal. Chem.* **1986**, *204*, 31.
(10) Marcus, R. A. *Annu. Rev. Phys. Chem.* **1964**, *15*, 155.
(11) Gerischer, H. *Z. Phys. Chem. (Munich)* **1961**, *27*, 40.
(12) Lanzafame, J. M.; Palese, S.; Wang, D.; Miller, R. J. D.; Muenter, A. A. *J. Phys. Chem.* **1994**, *98*, 11021.
(13) Newton, M. D.; Sutin, N. *Annu. Rev. Phys. Chem.* **1984**, *35*, 437.
(14) Iwasita, T.; Schmickler, W.; Schultze, J. W. *J. Electroanal. Chem.* **1985**, *194*, 355.
(15) Lanzafame, J. M.; Miller, R. J. D.; Muenter, A. A.; Parkinson, B. A. *J. Phys. Chem.* **1992**, *96*, 2820.
(16) Wang, D.; Buontempo, J.; Li, Z. W.; Miller, R. J. D. *Chem. Phys. Lett.* **1995**, *232*, 7.
(17) Rosenwaks, Y.; Thacker, B. R.; Ahrenkiel, R. K.; Nozik, A. J. *J. Phys. Chem.* **1992**, *96*, 10096.
(18) Viturro, R. E.; Woodall, J. M.; Wright, S. L.; Petit, G. D.; Shaw, J. L.; Kirchner, P. D.; Brillson, L. J. *J. Vac. Sci. Technol. B* **1988**, *6*, 1397.
(19) Sze, S. M. *Semiconductor Devices: Physics and Technology;* Wiley: New York, 1981.
(20) Hsiang, T. Y.; Zhou, X.; Miller, R. J. D. *J. Appl. Phys.* **1989**, *66*, 3066.
(21) Gomez-Jahn, L. A.; Miller, R. J. D. *J. Chem. Phys.* **1992**, *96*, 3982.
(22) (a) Beck, S. M.; Wessel, J. E. *Appl. Phys. Lett.* **1987**, *50*, 149. (b) Offsey, S. D.; Woodall, J. M.; Warren, A. C.; Kirchner, P. D.; Chappel, T. I.; Pettit, G. D. *Appl. Phys. Lett.* **1986**, *48*, 475.
(23) Knox, W. H.; Chemla, D. S.; Miller, D. A. B.; et al. *Phys. Rev. Lett.* **1989**, *62*, 503.
(24) Miller, D. A. B.; Chemla, D. S.; Damen, T. C.; et al. *Phys. Rev. Lett.* **1984**, *53*, 2173.
(25) Schneider, H.; Klitzing, K. V. *Phys. Rev. B* **1988**, *38*, 6160.
(26) Wang, S. *Fundamentals of Semiconductor Theory and Device Physics*; Prentice-Hall: Englewood Cliffs, NJ, 1989.
(27) Spiegel, M. R. *Theory and Problems of Advanced Mathematics for Engineers and Scientists*; McGraw-Hill Book Co.: New York, 1983.
(28) (a) Salcedo, J. R.; Siegman, A. E.; Dlott, D. D.; Fayer, M. D. *Phys. Rev. Lett.* **1978**, *41*, 131. (b) Einstein, A. *Investigations on the Theory of Brownian Movement;* Dover: New York, 1956.
(29) Wilkinson, G.; Stone, F. G. A.; Abel, E. W. *Comprehensive Organometallic Chemistry;* Pergamon Press: New York, 1982.
(30) (a) Smalley, J. F.; Feldberg, S. W.; Chidsey, C. D. E.; Linford, M. R.; Newton, M. D.; Liu, Y.-P *J. Phys. Chem.* **1995**, *99*, 13141. (b) Becka, A. M.; Miller, C. J. *J. Phys. Chem.* **1992**, *96*, 2657. (c) Guo, L. H.; Facci, J. S.; McLendon, G. *J. Phys. Chem.* **1995**, *99*, 8458.
(31) Chidsey, C. D. E. *Science* **1991**, *251*, 919.
(32) Miller, C.; Cuendet, P.; Grätzel, M. *J. Phys. Chem.* **1991**, *95*, 877.
(33) Weber, K.; Hockett, L.; Creager, S. *J. Phys. Chem. B* **1997**, *101*, 8286.
(34) Boudreaux, D. S.; Williams, F.; Nozik, A. J. *J. Appl. Phys*. **1980**, *51*, 2158.
(35) Ross, R. T.; Nozik, A. J. *J. Appl. Phys*. **1982**, *53*, 3813.
(36) (a) Lewis, N. S. *Annu. Rev. Phys. Chem.* **1991**, *42*, 543. (b) Fajardo, A. M.; Lewis, N. S. *Science* **1996**, *274*, 969.
(37) Maroncelli, M. *J. Mol. Liq*. **1993**, *57*, 1.
(38) Schmuttenmaer, C. A.; Miller, C. C.; Herman, J. W.; Cao, J.; Mantell, D. A.; Gao, Y.; Miller, R. J. D. *Chem. Phys.* **1996**, *205*, 91.
(39) (a) Diol, S. J.; Xu, S.; Gao, Y.; Miller, R. J. D., to be submitted. (b) Diol, S. J.; Miller, C. C.; Schmuttenmaer, C. A.; Cao, J.; Gao, Y.; Mantell, D. A.; Miller; R. J. D. *J. Phys. D* **1997**, *30*, 1427.
(40) Zhou, X. L.; Zhu, X. Y.; White, J. M. *Surf. Sci. Rep.* **1991**, *13*, 73.
(41) Schmuttenmaer, C. A.; Aeschlimann, M.; Elsayed-Ali, H. E.; Miller, R. J. D.; Mantell, D. A.; Cao, J.; Gao, Y. *Phys. Rev. B* **1994**, *50*, 8957.
(42) Gould, I. R.; Young, R. H.; Moody, R. E.; Farid, S. *J. Phys. Chem.* **1991**, *95*, 2068.
(43) Hannapel, T.; Burfeindt, B.; Storck, W.; Willig, F. *J. Phys. Chem. B* **1997**, *101*, 6799.
(44) Tachibana, Y.; Moser, J. E.; Grätzel, M.; Klug, D. R.; Durrant, J. R *J. Phys. Chem.* **1996**, *100*, 20056.
(45) Rehm, J. M.; McLendon, G. L.; Nagasawa, Y.; Yoshihara, K.; Moser, J.; Grätzel, M. *J. Phys. Chem.* **1996**, *100*, 9577.
(46) Smith, B. B.; Nozik, A. J. *Chem. Phys.* **1996**, *205*, 47.
(47) Boroda, Y. G.; Voth, G. A. *J. Chem. Phys.* **1996**, *104*, 6168.
(48) Boroda, Y. G.; Calhoun, A.; Voth, G. A. *J. Chem. Phys.* **1997**, *107*, 8940.